3D Numerical Modeling of Soluble Surfactant at Fluidic Interfaces Based on the Volume-of-Fluid Method

A. Alke[1] and D. Bothe[1]

Abstract: We present a computational approach based on the Volume-of-Fluid (VOF) method for simulating the influence of a soluble surfactant on the behavior of two-phase systems with deformable interface. Our approach is applicable to diffusion controlled processes, where the relation between the area-specific excess surfactant concentration on the interface and the volume-specific concentration adjacent to the interface is given by an adsorption isotherm. Main issues of the numerical model are an extended surface transport theorem used for describing the interfacial flux and an iso-surface of the VOF-variable used as a connected approximation for the interface. 3D-simulations of a bubble moving through a surfactant solution show the formation of a monotone concentration profile along the bubble surface with a surfactant-rich zone at the bubble's rear end. This is accompanied by regions of depleted and increased surfactant concentration in the bulk phase due to adsorption and desorption, respectively. The rise velocity reflects the retardation effect known from experiments.

Keywords: Soluble Surfactant, Two-Phase Flow, VOF - Simulation, Surface transport theorem.

1 Introduction

In many two-phase fluid-liquid systems, surface active agents (*surfactants* for short) are present either as impurities or as additives. Important examples include emulsification processes, where a surfactant is used to prevent droplet coalescence, and bubbly flows in bubble columns with contaminated water. A surfactant is preferentially adsorbed at the interface and reduces the surface tension, depending on its area specific excess concentration. The local surface tension is then given by a surface equation of state. The distribution of the adsorbed surfactant at the interface is determined by the flow conditions near the interface, the molecular transport of

---

[1] Center of Smart Interfaces, Mathematical Modeling and Analysis, Technical University of Darmstadt, Germany

the surfactant in the bulk phase and on the interface, and additionally by the sorption kinetics, unless bulk diffusion is the limiting factor. This distribution typically leads to a surface gradient of the surface tension, which has to be considered in the interfacial momentum jump condition. This additional Marangoni stress can result in a pronounced change of the dynamical behavior of fluid particles.

The hydrodynamic effect of surfactants on fluidic interfaces, especially for fluid particles, has been studied experimentally, analytically and numerically since the beginning of the second half of the 20th century. Starting point was the purely hydromechanical stagnant cap model developed by Savic (1953) for a spherical, steadily rising bubble contaminated with an insoluble surfactant. Later on, this model was improved concerning the mathematical solution procedure (Davis and Acrivos, 1966) and extended concerning a detailed mass balance of insoluble and soluble surfactant and deformability of the fluid particle; see, e.g., (Wasserman and Slattery, 1969; Harper, 1973; Levan and Newman, 1976; Harper, 1982; He, Malsrelli, and Dagan, 1990). Let us note that surfactants do not only alter the surface tension but also cause interfacial shear as well as dilatational viscosity; see, e.g., (Edwards, Brenner, and Wasan, 1991; Slattery, Sagis, and Oh, 2007). In (Khattari, Steffen, and Fischer, 2002), the influence of a surfactant on the migration of a spherical droplet is described, accounting for these additional interfacial properties. For the simulation of fluid particle deformation in the Stokes flow, the boundary integral method, see, e.g., (Pozrikidis, 2001), has been established, in which the flow field is obtained by solving an integral equation in which the interfacial momentum jump condition - expressing the pressure jump at a curved interface, and the Marangoni stresses in case of non-constant surface tension - are incorporated. The simultaneous surfactant transport is solved by using a Finite Difference method, e.g., (Milliken, Stone, and Leal, 1993; Li and Mao, 2001; Johnson and Borhan, 1996; Li and Pozrikidis, 1997), or a Finite Volume method, e.g., (Bazhlekov, Anderson, and Meijer, 2004, 2006), or a Finite Element approach (Feigl, Megias-Alguacil, Fischer, and Windhab, 2007). The latter three papers present 3D simulations whereas the others are restricted to axisymmetric shapes. In (Liao, Franses, and Barasan, 2003; Kruijt-Stegeman, van de Vosse, and Meijer, 2004; Severino, Campana, and Giavedoni, 2005) the Finite Element method is also employed for the numerical computation of the flow field. Except for (Johnson and Borhan, 1996; Severino, Campana, and Giavedoni, 2005), all the papers mentioned so far consider insoluble surfactants.

Recently, numerical methods capable of solving the full two-phase Navier-Stokes equations have been extended to simulate the influence of surfactant on the dynamical behavior of free interfaces. The methods of Yamamoto, Yamauchi, and Uemura (2006) and Zhang, Eckmann, and Ayyaswamy (2006) for deformable axisymmetric

particles are based on the front tracking method. The first one is limited to insoluble surfactants whereas the latter can also treat soluble surfactants. Muradoglu and Tryggvason (2008) presented a Finite-Difference/Front-Tracking method for axisymmetric flow with soluble surfactants. This method has recently been applied to a droplet cleavage induced by surfactant and to a buoyancy-driven rising bubble using a linear surface equation of state (Muradoglu and Tryggvason, 2008) as well as a nonlinear one (Tasoglu, Demirci, and Muradoglu, 2008). The model of Xu, Li, Lowengrub, and Zhao (2006) for 2D simulation of the influence of an insoluble surfactant on the droplet behavior, accounting for surface diffusion, relies on a Level-Set method and is applied to situations with a density and a viscosity ratio of one.

Renardy, Renardy, and Cristini (2002) and Drumright-Clarke and Renardy (2004) developed a VOF-based method to investigate the influence of an insoluble surfactant on the dynamical behavior in a 2D shear field. In this method the adsorbed surfactant is present only inside a layer enclosing the interface which is defined by two additional phase indicator functions. James and Lowengrub (2004) introduced a further VOF-based 2D method for insoluble surfactant in which the evolution of interfacial area and of the extensive quantity of surfactant mass are computed separately. Davidson and Harvie (2007) incorporated the method of James and Lowengrub into the VOF algorithm of Rudman (1998) and investigated transient axisymmetric deformations of a drop rising in a liquid. Yang and James (2007) developed an additional variant coupling the Level-Set and VOF techniques and taking advantage of the strengths of both parent methods. By directly tracking the surfactant mass, such hybrid method was shown to conserve surfactant mass and prevent surfactant from diffusing off the interface. The surfactant concentration, which determines the local surface tension through an equation of state, was computed as surfactant mass per interfacial area.

In the present paper, a VOF-based method for simulating the influence of a soluble surfactant on the behavior of two-phase systems with deformable interface due to Marangoni stresses is introduced. This approach is applicable to diffusion controlled processes, where the relation between the area-specific excess surfactant concentration on the interface and the volume-specific concentration adjacent to the interface is given by an adsorption isotherm. Our aim here is to show the principal feasibility of the method. The remainder of this paper is organized as follows. In Section 2, the governing equations based on continuum mechanics are given. In Section 3, the numerical model based on the VOF-method is described in detail. In Section 4, first numerical results for a bubble rising in a surfactant solution are presented. Section 5 gives final conclusions. This paper is based on (Alke and Bothe, 2007) and (Alke, 2008).

2   The governing equations

We consider a two-phase system consisting of a surfactant solution (phase domain $\Omega^+(t)$) and a fluid phase in which the surfactant is insoluble (phase domain $\Omega^-(t)$). The deformable interface between the two phases is presented as a (sharp) surface of zero thickness and is denoted by $\Sigma(t)$. Furthermore, the following assumptions are imposed:

- a dilute surfactant solution (bulk concentration below critical micelle concentration) without interaction between adsorbed surfactant molecules,

- chemically inert surfactant,

- no phase change,

- isothermal conditions,

- incompressible bulk phases.

The present paper employs a continuum mechanical model in which the governing equations are based on the conservation of surfactant (molar) mass, mass and momentum. Since no chemical reaction and no surfactant flux across the boundary of the domain occur, the total surfactant mass - that is the surfactant mass which is either adsorbed on the interface or dissolved in the bulk phase $\Omega^+(t)$ - is constant. In the local formulation, the balance equations for surfactant mass read as

$$\frac{Dc}{Dt} + \nabla \cdot \mathbf{j} = 0 \quad \text{in} \quad \Omega^+(t), \quad c = 0 \quad \text{in} \quad \Omega^-(t) \tag{1}$$

inside the bulk phases, and (Edwards, Brenner, and Wasan, 1991)

$$\frac{D\Gamma}{Dt} + \Gamma \, \nabla_\Sigma \cdot \mathbf{u} + \nabla_\Sigma \cdot \mathbf{j}^\Sigma = r^{ad} - r^{de} \quad \text{on} \quad \Sigma(t) \tag{2}$$

where $\frac{D}{Dt}$ is the Lagrangian derivative. Here c is the volume specific molar concentration of the dissolved surfactant, Γ denotes the area specific molar excess concentration of the adsorbed surfactant, $\mathbf{j}$ and $\mathbf{j}^\Sigma$ are the volumetric and interfacial diffusive fluxes, respectively, and r^{ad} and r^{de} are the rate functions for adsorption and desorption, respectively. Common rate laws which are applicable to most surfactants are, according to Langmuir, $r^{ad} = k_{ad} \, (1 - \Theta) \, c$ and $r^{de} = k_{de} \Theta$ with the adsorption rate constant k_{ad} and the desorption rate constant k_{de}. For the molecular fluxes $\mathbf{j}$ and $\mathbf{j}^\Sigma$ suitable constitutive model equations have to be chosen. In case of dilute systems and negligible interactions between adsorbed molecules, Fick's law

$$\mathbf{j} = -D \, \nabla c, \tag{3}$$

and

$$\mathbf{j}^{\Sigma} = -D^{\Sigma}\,\nabla_{\Sigma}\Gamma, \tag{4}$$

with diffusion coefficients D and D^{Σ} and the surface gradient $\nabla_{\Sigma}\Gamma$ are appropriate. Note that for bulk concentrations larger than the critical micelle concentration, a source term accounting for the micellar composition and decomposition would be required in (1). The two balance equations (1) and (2) are coupled via the interfacial transmission condition

$$r^{ad} - r^{de} + \mathbf{j}_{|\Sigma}\cdot\mathbf{n}_{\Sigma} = 0, \tag{5}$$

where $\mathbf{j}_{|\Sigma}$ is the one-sided limit of the molecular bulk flux. In (5), as in the remainder of the present paper, the interfacial normal unit vector $\mathbf{n}_{\Sigma}$ is always directed into $\Omega^{+}(t)$. Because of (5), knowledge about the sorption kinetics is required for the correct interfacial transmission condition of the surfactant bulk transport equation. For the further treatment the following two additional assumptions are imposed

- local thermodynamical equilibrium at the interface,

- no surface viscosities.

The first of these two assumptions limits the applicability of the model to the important class of diffusion controlled adsorption processes. In this case of fast sorption compared to diffusion local thermodynamical equilibrium holds at the interface. Hence a sorption isotherm, given as $\Gamma = g(c_{|\Sigma})$, holds on the interface, where $c_{|\Sigma}$ is the bulk concentration adjacent to the interface. The assumption of quasi-instantaneous sorption is valid for a large number of surfactants (Ravera, Ferrari, and Liggieri, 2000), mainly for those with a low molecular weight. For such low weight surfactants surface viscosity effects can be neglected, in general. The most commonly used equilibrium relation is the Langmuir isotherm (resulting from the Langmuir rate laws mentioned above), given by

$$\frac{\Gamma}{\Gamma_{\infty}} = \frac{c_{|\Sigma}}{c_{|\Sigma} + b}; \tag{6}$$

here b is the Langmuir coefficient representing the ratio k_{de}/k_{ad} of the rate constants for desorption and adsorption, and Γ_{∞} is the maximum interfacial concentration of surfactant.

The underlying velocity field is governed by the two-phase Navier-Stokes equations expressing conservation of mass and momentum. Assuming continuity of

the velocity at the interface for viscous (Newtonian) fluids of constant density, the one-field formulation reads as

$$\nabla \cdot \mathbf{u} = 0 \tag{7}$$

and

$$\rho \frac{D\mathbf{u}}{Dt} = -\nabla p + \nabla \cdot \mathbf{S} + \rho \mathbf{g} + (\sigma \, \kappa \, \mathbf{n}_\Sigma + \nabla_\Sigma \sigma) \, \delta_\Sigma, \tag{8}$$

where $\mathbf{S}$ denotes the viscous stress tensor, i.e.

$$\mathbf{S} = \eta \left(\nabla \mathbf{u} + (\nabla \mathbf{u})^\mathsf{T} \right). \tag{9}$$

Here the material properties ρ and η refer to the phase dependent values, i.e.

$$\rho = f\rho^+ + (1-f)\rho^- \tag{10}$$

and

$$\eta = f\eta^+ + (1-f)\eta^-, \tag{11}$$

where f is the phase indicator function of the phase domain $\Omega^+(t)$. In (8), the momentum jump conditions are incorporated via the interfacial Delta distribution δ_Σ. The first term in brackets on the right-hand side of (8) contains the curvature $\kappa = -\nabla \cdot \mathbf{n}_\Sigma$ (more precisely, the sum of the principal curvatures) and expresses the Laplace pressure jump. The surface gradient of the surface tension corresponds to the Marangoni stress. Under isothermal conditions, this surface gradient is due to local variations of Γ. For a given surface equation of state, $\sigma = \sigma(\Gamma)$, the Marangoni stress is determined by the distribution of adsorbed surfactant according to

$$\nabla_\Sigma \sigma(\Gamma) = \frac{d\sigma}{d\Gamma} \nabla_\Sigma \Gamma. \tag{12}$$

For more details on continuum mechanical modelling of two-phase fluidic systems see, e.g., (Edwards, Brenner, and Wasan, 1991; Slattery, Sagis, and Oh, 2007). For first results on the mathematical analysis concerning wellposedness of the above model for two-phase flow with soluble surfactant see (Bothe, Prüss, and Simonett, 2005).

3   Numerical model for transport of soluble surfactant

3.1   *Finite Volume approach*

To solve the equations given above numerically, we use the commercial CFD-solver FLUENT employing the Finite Volume discretization and especially a VOF-method to solve the two-phase Navier-Stokes system. Within the VOF-method, the interface is implicitly captured by solving the transport equation

$$\frac{\partial f}{\partial t} + \nabla \cdot (f\mathbf{u}) = 0 \tag{13}$$

for the phase indicator function. In the context of the Finite Volume discretization, the volume averaged value of f corresponds to the volume fraction of phase Ω^+ within a computational cell. For the discretization of the convective term of (13), several schemes are available in FLUENT. To minimize artificial smearing of the VOF-variable f, the tracking algorithm as described in (Youngs, 1982) employing geometrical calculation of the fluxes is chosen. Here, for each interface carrying cell, the interface is locally approximated by a plane, so that a conservative transport of the phase volume without numerical diffusion is ensured. The surface tension force is incorporated as a volume force according to the Continuum Surface Force (CSF) model (Brackbill, Kothe, and Zemach, 1992).

Based on this VOF-method, a numerical scheme for the surfactant transport is developed. Here especially those computational cells containing a part of the interface are of interest. The total surfactant (molar) mass N in a cell at time t^{n+1} is computed in an explicit manner as

$$N(t^{n+1}, V \cap \Omega^+(t^{n+1})) = N(t^n, V \cap \Omega^+(t^n)) + \Delta t \dot{N}(t^n), \tag{14}$$

with $t^{n+1} = t^n + \Delta t$. The rate of change of total surfactant (molar) mass $\dot{N}$ inside a fixed control volume is (see Appendix B, equation (46))

$$\dot{N} = \frac{d}{dt}\left[\int_{V \cap \Omega^+(t)} c\, dV + \int_{\Sigma(t) \cap V} \Gamma\, dA\right] = -\int_{\partial V \cap \Omega^+(t)} (c\, \mathbf{u} + \mathbf{j}) \cdot \mathbf{n}\, dA$$

$$-\int_{\partial(\Sigma(t) \cap V)} \mathbf{j}^\Sigma \cdot \mathbf{N}\, ds - \int_{\partial(\Sigma(t) \cap V)} \Gamma\, \frac{\mathbf{u} \cdot \mathbf{n}}{\sqrt{1 - (\mathbf{n}_\Sigma \cdot \mathbf{n})^2}}\, ds. \tag{15}$$

The first term on the right-hand side of equation (15) describes the convective and molecular bulk transport of the dissolved surfactant across the cell faces which lie inside the bulk phase Ω^+. The second term accounts for the surface diffusion of the adsorbed surfactant across the intersection curve between the interface and the

cell boundary. The last term describes the transported adsorbed surfactant into or out of the control volume due to interface movement.

To calculate the rate (15) numerically, we employ a kind of operator splitting. A special feature within the VOF method of FLUENT is the possibility to solve transport equations for user defined scalars within one of the phases, but without transfer across the interface, i.e. with the homogeneous Neumann boundary condition

$$\mathbf{j} \cdot \mathbf{n}_\Sigma = 0 \quad \text{on} \quad \Sigma(t). \tag{16}$$

This is used to solve equation (1), i.e. for the pure bulk transport of dissolved surfactant inside Ω^+. Note that condition (16) does not reflect the physics of adsorption since it does not allow diffusive transport of dissolved surfactant to or from the interface. Let $\widetilde{c}$ denote the resulting bulk concentration. Then, since quasi-instantaneous sorption is assumed, relation (6) is used to compute the surface concentration as $g(\widetilde{c})$ inside the interfacial cells. This leads to an intermediate value $\widetilde{N}^{n+1} := \widetilde{N}(t^{n+1}, V \cap \Omega^+(t^{n+1}))$ given by

$$\widetilde{N}^{n+1} = \left[\int_{V \cap \Omega^+(t^{n+1})} \widetilde{c}\, dV + \int_{\Sigma(t^{n+1}) \cap V} g(\widetilde{c})\, dA \right]_{\mathbf{j} \cdot \mathbf{n}_\Sigma = 0}. \tag{17}$$

Here the notation $[\dots]_{\mathbf{j} \cdot \mathbf{n}_\Sigma = 0}$ is used to indicate that the quantity inside the brackets is computed using the boundary condition (16) instead of the true boundary condition

$$-\mathbf{j} \cdot \mathbf{n}_\Sigma = \frac{D\Gamma}{Dt} + \Gamma\, \nabla_\Sigma \cdot \mathbf{u} + \nabla_\Sigma \cdot \mathbf{j}^\Sigma \quad \text{on} \quad \Sigma(t) \tag{18}$$

which results from (2) and (5). To compute the correct value N^{n+1} from $\widetilde{N}^{n+1}$, we use the fact that

$$\widetilde{N}^{n+1} \doteq N^n + \Delta t \left(\frac{d}{dt} \left[\int_{V \cap \Omega^+(t)} \widetilde{c}\, dV + \int_{\Sigma(t) \cap V} g(\widetilde{c})\, dA \right]_{\mathbf{j} \cdot \mathbf{n}_\Sigma = 0} \right). \tag{19}$$

An appropriate reformulation of the rate term in (19) (cf. Appendix C, equation (51)) yields

$$\frac{d}{dt} \left[\int_{V \cap \Omega^+(t)} \widetilde{c}\, dV + \int_{\Sigma(t) \cap V} g(\widetilde{c})\, dA \right]_{\mathbf{j} \cdot \mathbf{n}_\Sigma = 0} = - \int_{\partial V \cap \Omega^+(t)} \left(\widetilde{c}\, \mathbf{u} + \widetilde{\mathbf{j}} \right) \cdot \mathbf{n}\, dA$$

$$+ \int_{\Sigma(t) \cap V} \left(\frac{D}{Dt} g(\widetilde{c}) + g(\widetilde{c}) \nabla_\Sigma \cdot \mathbf{u} \right) dA - \int_{\partial(\Sigma(t) \cap V)} g(\widetilde{c}) \frac{\mathbf{u} \cdot \mathbf{n}}{\sqrt{1 - (\mathbf{n}_\Sigma \cdot \mathbf{n})^2}}\, ds. \tag{20}$$

To calculate the total molar surfactant mass N^{n+1} with the help of (20), the differences between the right-hand sides of equations (15) and (20) have to be accounted

for by an additional source term $\dot{S}$. An elementary calculation (cf. Appendix C) yields

$$\frac{d}{dt}\left[\int_{V\cap\Omega^+(t)} c\,dV + \int_{\Sigma(t)\cap V}\Gamma\,dA\right] = $$
$$\frac{d}{dt}\left[\int_{V\cap\Omega^+(t)}\widetilde{c}\,dV + \int_{\Sigma(t)\cap V}g(\widetilde{c})\,dA\right]_{\mathbf{j}\cdot\mathbf{n}_\Sigma=0} + \dot{S}(\widetilde{c}) \tag{21}$$

with

$$\dot{S}(\widetilde{c}) = -\int_{\partial(\Sigma(t)\cap V)}\mathbf{j}^\Sigma\cdot\mathbf{N}\,ds - \int_{\Sigma(t)\cap V}\left(\frac{D}{Dt}g(\widetilde{c}) + g(\widetilde{c})\nabla_\Sigma\cdot\mathbf{u}\right)dA. \tag{22}$$

This finally yields N^{n+1} according to

$$N^{n+1} = \widetilde{N}^{n+1} + \Delta t\,\dot{S}(\widetilde{c}). \tag{23}$$

In the Finite Volume discretization, (17) corresponds to

$$\widetilde{N}_i^{n+1} = \widetilde{c}_i^{n+1}\left|V_i\cap\Omega^+(t^{n+1})\right| + g(\widetilde{c}_i^{n+1})\left|A_{\Sigma,i}(t^{n+1})\right|, \tag{24}$$

where V_i is a grid cell and $\widetilde{c}_i^{n+1}$ the cell centered value of $\widetilde{c}$, $\left|V_i\cap\Omega^+(t^{n+1})\right|$ denotes the part of V_i lying inside Ω^+ and $\left|A_{\Sigma,i}(t^{n+1})\right|$ the area of the interface inside the computational cell V_i at time t^{n+1}. Next, the value N_i^{n+1} is computed according to (23). Finally, the values c_i^{n+1} and Γ_i^{n+1} are obtained from the relations

$$N_i^{n+1} = c_i^{n+1}\left|V_i\cap\Omega^+(t^{n+1})\right| + \Gamma_i^{n+1}\left|A_{\Sigma,i}(t^{n+1})\right| \tag{25}$$

and

$$\Gamma_i^{n+1} = g(c_i^{n+1}). \tag{26}$$

With this approach no separate area concentrations of the adsorbed surfactant are required and only bulk values need to be stored.

It remains to provide a reformulation of $\dot{S}$ from (22) which is feasible for subsequent discretization. Applying the balance equation (1) to the Lagrangian derivative of the function $g(\widetilde{c})$, the source term (22) takes the form

$$\dot{S} = -\int_{\partial(\Sigma(t)\cap V)}\mathbf{j}^\Sigma\cdot\mathbf{N}\,ds + \int_{\Sigma(t)\cap V}g'(\widetilde{c})\nabla\cdot\mathbf{j}\,dA - \int_{\Sigma(t)\cap V}g(\widetilde{c})\,\nabla_\Sigma\cdot\mathbf{u}\,dA. \tag{27}$$

With the homogeneous Neumann boundary condition (16), the divergence in the second term of (27) reduces to the surface divergence. Employing (3) with constant diffusivity for the molecular flux, the Langmuir isotherm (6) for the function

g and some mathematical rearrangements using especially the surface divergence theorem, it follows that

$$
\begin{aligned}
\dot{S} = \ &- \int_{\partial(\Sigma(t)\cap V)} \mathbf{j}^{\Sigma} \cdot \mathbf{N}\, ds - \int_{\partial(\Sigma(t)\cap V)} D\, \nabla_{\Sigma} g(\widetilde{c}) \cdot \mathbf{N}\, ds \\
&- \int_{\Sigma(t)\cap V} \frac{2(b+\widetilde{c})}{\Gamma_{\infty} b} D \, \|\nabla_{\Sigma} g(\widetilde{c})\|^2 \; dA + \int_{\Sigma(t)\cap V} \mathbf{u}_{\tau} \cdot \nabla_{\Sigma} g(\widetilde{c}) \; dA \\
&- \int_{\partial(\Sigma(t)\cap V)} g(\widetilde{c})\, \mathbf{u}_{\tau} \cdot \mathbf{N}\, ds + \int_{\Sigma(t)\cap V} g(\widetilde{c})\, \kappa\, \mathbf{u} \cdot \mathbf{n}_{\Sigma}\, dA.
\end{aligned}
\tag{28}
$$

Here, the first term accounts for the surface diffusion. The second and third term subtract the unphysical flux induced by the bulk transport. The remaining terms result from the dilation or compression of the interface due to movement in tangential (fourth, resp. fifth term) and normal (sixth term) direction. Figure 1 summarizes the main steps of the computations in every time step. The numerical discretization of (28) requires a connected approximation of the interface. The standard PLIC scheme does not fulfill this requirement, but a connected interface approximation can be obtained as described in the next section as an f-iso-surface.

3.2   *Construction of an iso-surface for the VOF-variable*

The discretization of the terms in (28) is based on an iso-surface Σ_{iso} concerning the VOF-variable f as an approximation of the true interface $\Sigma(t)$. Figure 2 shows the steps of the construction of this iso-surface. Figure 3 shows the possible configurations of the iso-surface inside a cubic cell. In the first step, VOF-values f_{node} at all grid nodes are determined by volume averaging over the cell center values of the adjoining cells. Next, the coordinates of the intersection points $\mathbf{x}_s \in \Sigma_{iso}$ with the edges of the grid are calculated for a given VOF-value f_{iso}. This is done by linear interpolation of the f-values along the edges. For the case of more than three edge/iso-surface intersections, the latter are, in general, not in a plane. Therefore, the part $\Sigma_{iso,i}$ of the iso-surface lying inside the cell V_i is triangulated by connecting each edge/iso-surface-intersection point with the center point (given as the arithmetic mean of all associated intersection points). The phase volume fraction in a grid cell resulting from the phase partitioning by the iso-surface does not coincide with the cell centered value of the VOF-variable, so that this process does not conserve phase volume. However, these deviations cannot accumulate since the PLIC-algorithm is still used for the f-transport while the iso-surface is used in each time step as the basis for the interfacial surfactant transport.
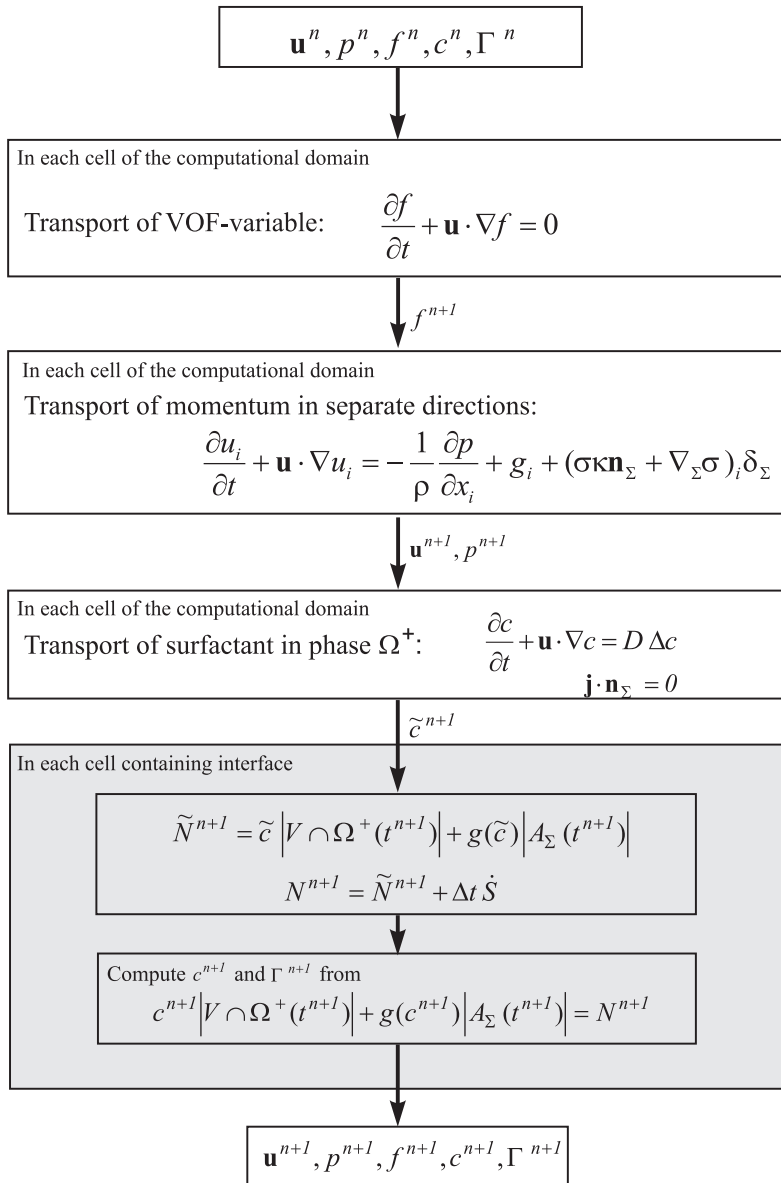
$$\boxed{\mathbf{u}^n, p^n, f^n, c^n, \Gamma^n}$$

In each cell of the computational domain

Transport of VOF-variable: $\dfrac{\partial f}{\partial t} + \mathbf{u} \cdot \nabla f = 0$

f^{n+1}

In each cell of the computational domain

Transport of momentum in separate directions:

$$\frac{\partial u_i}{\partial t} + \mathbf{u} \cdot \nabla u_i = -\frac{1}{\rho}\frac{\partial p}{\partial x_i} + g_i + (\sigma \kappa \mathbf{n}_\Sigma + \nabla_\Sigma \sigma)_i \delta_\Sigma$$

$\mathbf{u}^{n+1}, p^{n+1}$

In each cell of the computational domain

Transport of surfactant in phase Ω^+: $\quad \dfrac{\partial c}{\partial t} + \mathbf{u} \cdot \nabla c = D\,\Delta c$

$\mathbf{j} \cdot \mathbf{n}_\Sigma = 0$

$\widetilde{c}^{n+1}$

In each cell containing interface

$$\widetilde{N}^{n+1} = \widetilde{c}\left| V \cap \Omega^+(t^{n+1}) \right| + g(\widetilde{c})\left| A_\Sigma(t^{n+1}) \right|$$

$$N^{n+1} = \widetilde{N}^{n+1} + \Delta t\,\dot{S}$$

Compute c^{n+1} and Γ^{n+1} from

$$c^{n+1}\left| V \cap \Omega^+(t^{n+1}) \right| + g(c^{n+1})\left| A_\Sigma(t^{n+1}) \right| = N^{n+1}$$

$$\boxed{\mathbf{u}^{n+1}, p^{n+1}, f^{n+1}, c^{n+1}, \Gamma^{n+1}}$$

Figure 1: Sequence of calculations in a single time step

a) distribution of f-values and non connected PLIC-construction

b) node values f_{node} by volume averaging over neighbouring cells

c) intersection points f_{iso} by linear interpolation of f_{node}-values

d) iso-surface by connecting of intersection points f_{Iso}
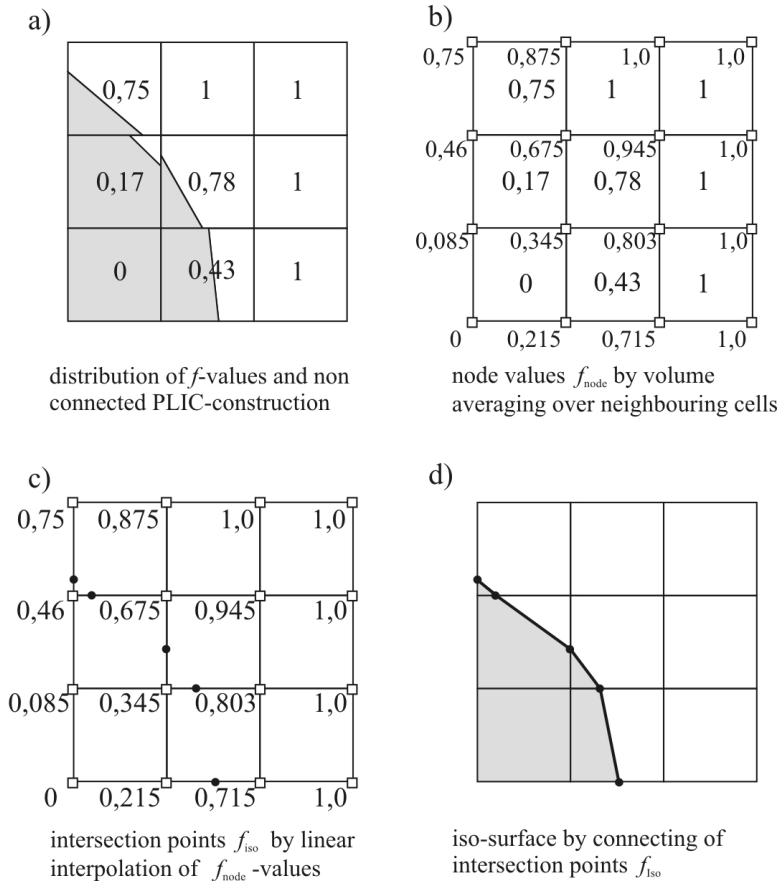
Figure 2: Algorithm for constructing the iso-surface $f_{iso} = const.$ from cell center values of the VOF-variable f

3.3 Interfacial source term

The first term in (28) describes the change of adsorbed surfactant inside a control volume due to surface diffusion along the interface $\Sigma(t)$. The cell specific value for Γ_i is calculated from the sorption isotherm $\Gamma_i = g(\widetilde{c}_i)$, where $\widetilde{c}$ is the bulk concentration of surfactant after bulk transport as explained in section 3.1. With Fick's law for surface diffusion (4) and the outward oriented tangential unit vector $\mathbf{N}_{nb} = \mathbf{x}_{c,nb} - \mathbf{x}_{c,i} / \|\mathbf{x}_{c,nb} - \mathbf{x}_{c,i}\|$, the discrete form of this term is given as

$$-\int_{\partial(\Sigma(t)\cap V_i)} \mathbf{j}^{\Sigma} \cdot \mathbf{N} ds = \int_{\partial(\Sigma(t)\cap V_i)} D^{\Sigma} \nabla_{\Sigma} \Gamma \cdot \mathbf{N} ds \approx \sum_{nb} D^{\Sigma} \frac{g(\widetilde{c}_{nb}) - g(\widetilde{c}_i)}{\|\mathbf{x}_{c,nb} - \mathbf{x}_{c,i}\|} |s_{i,nb}| \quad (29)$$
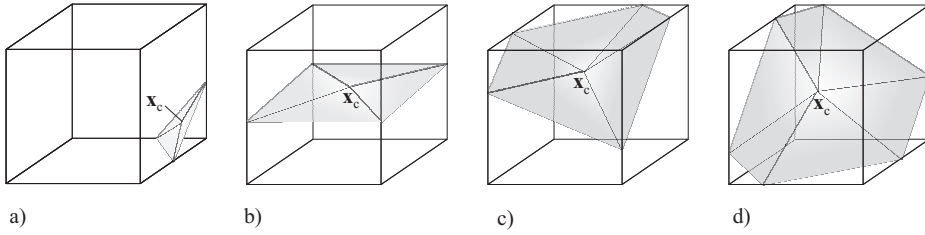
Figure 3: Possible locations of the iso-surface in a computational cell: *a*) three, *b*) four, *c*) five and *d*) six edge/iso-surface intersections
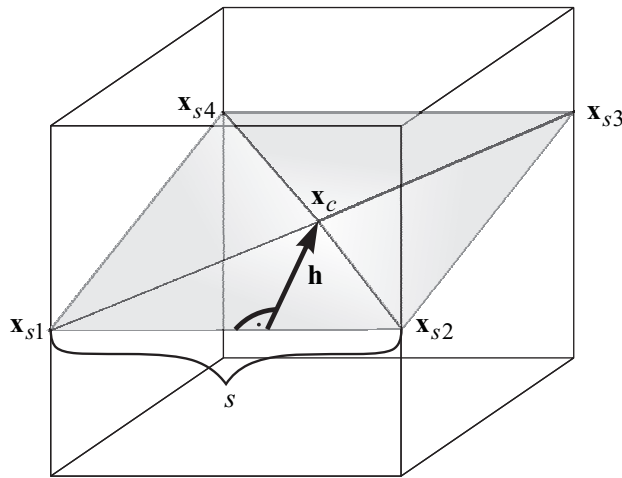

Figure 4: Geometrical quantities of the iso-surface

where $\sum_{nb}$ denotes the sum over all neighboring cells which are cut by iso-surface and $s_{i,nb}$ the line of intersection between the face $A_{i,nb}$ (belonging to cell V_i and V_{nb}) and the iso-surface Σ_{iso}. Here we assume a constant surface diffusion coefficient D^Σ. The discrete form of the second term in (28) has the same structure and, therefore, can be calculated together with (29). Furthermore, the tangential velocity $\mathbf{u}_\tau$ in the fourth and fifth term of (28) can be replaced by the full velocity $\mathbf{u}$. The latter as well as the concentration c and the equilibrium value $g(c)$ are given as cell specific values. However, for the fifth term the velocity $\mathbf{u}$ is needed at the intersection lines $s_{i,nb}$ which is obtained by linear interpolation. The unit vector $\mathbf{N}$ is calculated according to $\mathbf{N} = -\mathbf{h}/\|\mathbf{h}\|$, where $\mathbf{h}$ is the hight vector of the corresponding trian-

gle; cf. Figure 4 for an example with vortices $\mathbf{x}_{s,1}, \mathbf{x}_{s,2}$ and $\mathbf{x}_c$. In addition, for the third and fourth term the surface gradient $\nabla_\Sigma g(\widetilde{c})$ is needed as a cell specific value. In section 3.4 it is described in detail how to approximate this value. Furthermore, to be able to discretize the sixth term which contains the curvature, the relation $\int \mathbf{N}\, ds = \int d\mathbf{s} \times \mathbf{n}_\Sigma = \int \kappa\, \mathbf{n}_\Sigma\, dA$ is employed. To achieve a certain smoothing of the curvature term in this expression, the tangential unit vector $\mathbf{N}$ is calculated in the same manner as in the surface diffusion term, i.e. from the distance vector between two iso-surface centers $\mathbf{x}_c$. Altogether, the discrete Finite Volume version of the interfacial source term becomes

$$
\begin{aligned}
\dot{S}_i^{discrete} = \quad & \left(D^\Sigma - D\right) \sum_{nb} \frac{g(\widetilde{c}_i) - g(\widetilde{c}_{nb})}{\|\mathbf{x}_{c,i} - \mathbf{x}_{c,nb}\|}\, |s_{i,nb}| \\[2mm]
- \quad & \frac{2(b + \widetilde{c}_i)}{\Gamma_\infty b} D\, \|\nabla_\Sigma g(\widetilde{c})\|_i^2\, |A_{\Sigma,i}| + \mathbf{u}_i \cdot (\nabla_\Sigma g(\widetilde{c}))_i\, |A_{\Sigma,i}| \\[2mm]
- \quad & g(\widetilde{c}_i) \sum_{nb} \mathbf{u}_{i,nb} \cdot \left(-\frac{\mathbf{h}_{i,nb}}{\|\mathbf{h}_{i,nb}\|}\right)\, |s_{i,nb}| \\[2mm]
+ \quad & g(\widetilde{c}_i)\, \mathbf{u}_i \cdot \sum_{nb} \frac{\mathbf{x}_{c,nb} - \mathbf{x}_{c,i}}{\|\mathbf{x}_{c,nb} - \mathbf{x}_{c,i}\|}\, |s_{i,nb}|\,.
\end{aligned}
\tag{30}
$$

3.4 Cell specific surface gradient

In this subsection the calculation of the surface gradient of $g(\widetilde{c})$ appearing in (30) as well as in the discrete version of the Marangoni stress term (12) is described. In local coordinates, the surface gradient of a surface quantity ϕ^Σ is defined as

$$
\nabla_\Sigma \phi^\Sigma = \frac{\partial \phi^\Sigma}{\partial \boldsymbol{\tau_1}} \boldsymbol{\tau}_1 + \frac{\partial \phi^\Sigma}{\partial \boldsymbol{\tau_2}} \boldsymbol{\tau}_2,
\tag{31}
$$

where $\boldsymbol{\tau_1}$ and $\boldsymbol{\tau_2}$ are two orthogonal tangential unit vectors. To compute the directional derivatives $\frac{\partial \phi^\Sigma}{\partial \boldsymbol{\tau_i}}$, we proceed as follows. First, two linear independent approximately tangential vectors $\mathbf{t}_i$ are determined in a way which depends on the number of edge/iso-surface intersections (cf. Figure 5): If the computational cell contains three edge/iso-surface intersections, two spanning vectors of the triangle are used as tangential vectors (Figure 5a). In the case of four edge/iso-surface intersections, the diagonal vectors are used (Figure 5b). If the computational cell is cut by the iso-surface at five intersection points, the two end points of the shortest intersection line between a cell face and the iso-surface are replaced by one middle point. Then, the diagonal vectors obtained from the remaining four points are used as the tangential vectors $\mathbf{t}_i$ (Figure 5c). An analogous procedure is applied in
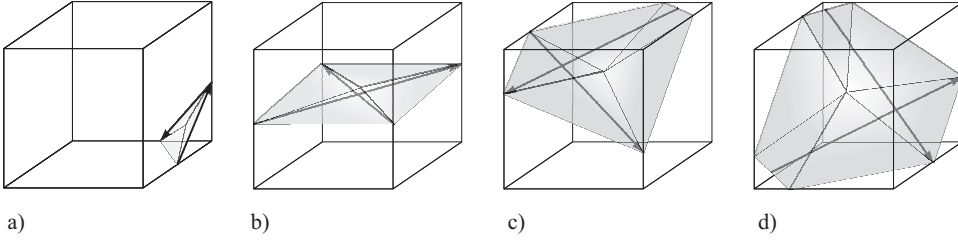
Figure 5: Determination of two linear independent vectors, which are approximately tangential at the interface; a) three, b) four, c) five, and d) six cell intersections

case of six edge/iso-surface intersections (Figure 5d). This yields (approximately) tangential orthogonal unit vectors

$$\boldsymbol{\tau}_1 = \frac{\mathbf{t}_1}{\|\mathbf{t}_1\|} \quad \text{and} \quad \boldsymbol{\tau}_2 = \frac{\mathbf{t}_1 \times (\mathbf{t}_2 \times \mathbf{t}_1)}{\|\mathbf{t}_1 \times (\mathbf{t}_2 \times \mathbf{t}_1)\|}. \tag{32}$$

Next, the directional derivatives $\frac{\partial \phi^{\Sigma}}{\partial \boldsymbol{\tau}_1}$ and $\frac{\partial \phi^{\Sigma}}{\partial \boldsymbol{\tau}_2}$ are approximated according to a least square method. On the discrete level, on each face of an interfacial cell the directional derivative $\frac{\partial \phi^{\Sigma}}{\partial \boldsymbol{\tau}_{nb}}$ in direction of the connecting line between the two points $\mathbf{x}_{c,nb}$ and $\mathbf{x}_{c,i}$ can be approximated by

$$\frac{\partial \phi^{\Sigma}}{\partial \boldsymbol{\tau}_{nb}} \approx \frac{\phi_{nb}^{\Sigma} - \phi_i^{\Sigma}}{\|\mathbf{x}_{c,nb} - \mathbf{x}_{c,i}\|}, \tag{33}$$

where the tangential unit vector is given as $\boldsymbol{\tau}_{nb} = \frac{\mathbf{x}_{c,nb} - \mathbf{x}_c}{\|\mathbf{x}_{c,nb} - \mathbf{x}_c\|}$. Therefore, an approximate cell specific surface gradient $\nabla_{\Sigma} \phi^{\Sigma}$ has to fulfill the requirement

$$\sum_{nb} \left(\left((\nabla_{\Sigma} \phi^{\Sigma}) \right)_i \cdot \boldsymbol{\tau}_{nb} - \frac{\phi_{nb}^{\Sigma} - \phi_i^{\Sigma}}{\|\mathbf{x}_{c,nb} - \mathbf{x}_{c,i}\|} \right)^2 \to \min! \tag{34}$$

This minimization problem has a unique solution, given by

$$\frac{\partial \phi^{\Sigma}}{\partial \boldsymbol{\tau}_1} = \frac{\sum_{nb} a_{2,nb}^2 \sum_{nb} a_{1,nb} b_{nb} - \sum_{nb} a_{1,nb} a_{2,nb} \sum_{nb} a_{2,nb} b_{nb}}{\sum_{nb} a_{1,nb}^2 \sum_{nb} a_{2,nb}^2 - \left(\sum_{nb} a_{1,nb} a_{2,nb} \right)^2}.$$

$$\frac{\partial \phi^{\Sigma}}{\partial \boldsymbol{\tau}_2} = \frac{\sum_{nb} a_{2,nb} b_{nb} - \frac{\partial \phi^{\Sigma}}{\partial \boldsymbol{\tau}_1} \sum_{nb} a_{1,nb} a_{2,nb}}{\sum_{nb} a_{2,nb}^2} \tag{35}$$

where $a_{1,nb} = \boldsymbol{\tau}_1 \cdot \frac{\mathbf{x}_{c,nb} - \mathbf{x}_{c,i}}{\left\| \mathbf{x}_{c,nb} - \mathbf{x}_{c,i} \right\|}$, $a_{2,nb} = \boldsymbol{\tau}_2 \cdot \frac{\mathbf{x}_{c,nb} - \mathbf{x}_{c,i}}{\left\| \mathbf{x}_{c,nb} - \mathbf{x}_{c,i} \right\|}$, and $b_{nb} = \frac{\phi_{nb}^{\Sigma} - \phi_i^{\Sigma}}{\left\| \mathbf{x}_{c,nb} - \mathbf{x}_{c,i} \right\|}$.

This procedure has been successfully tested and verified for prototype cases, and is used to compute the surface gradient of $g(\widetilde{c})$.

4 Application to a rising bubble

4.1 *Computational domain and physical parameters*

In this section a qualitative study of the effect of a soluble surfactant on the rise behavior of a bubble is presented. We consider a bubble of 2 mm volume-equivalent diameter rising in a 6 mm tube filled with a water/glycerol mixture (density: $\rho = 998.2\ kg/m^3$, viscosity: $\eta = 10\ mPa\ s$). According to Schlüter (2002), the trajectory of a gas bubble rising in a fluid with a viscosity of at least 7 $mPa\ s$ is rectilinear. Hence the simulation of a quarter of the bubble is sufficient. To realize a rotationally symmetric flow field a cylinder is chosen as the computational domain as shown in Figure 6. Since the present implementation of our numerical method requires rectangular computational cells, the computational domain is divided into a rectangular core zone which is discretized with cubic cells and a peripheral zone which is discretized with an unstructured grid as shown in Figure 7. The current restriction to rectangular cells is not a principle one and the approach can be adopted to tetrahedra, say, in a straightforward manner. The length of the computational domain is $L = 10\ mm$ and the radius is $R = 3\ mm$.

Concerning the momentum transport, the zero shear stress (slip) condition is applied at all domain boundaries to minimize the wall influence, i.e. the boundary conditions are

$$\mathbf{u} \cdot \mathbf{n} = 0 \quad \text{and} \quad (\mathbf{Sn}) \cdot \boldsymbol{\tau} = 0 \quad \text{on} \quad \partial \Omega. \tag{36}$$

Concerning the boundary condition for the surfactant transport equation, the homogeneous Neumann-boundary condition

$$\nabla c \cdot \mathbf{n} = 0 \quad \text{on} \quad \partial \Omega \tag{37}$$

is imposed at the whole domain boundary. The surfactant parameters used in our simulations are listed in Table 1. Since no reliable experimental data concerning the interfacial diffusion coefficient is available, we have chosen $D^{\Sigma} = 10^{-5} m^2 s^{-1}$ as a reasonable value. The values of the other coefficients in Table 1 correspond to the non ionic surfactant *Triton X 100* for which diffusion in the bulk phase is the rate determining step (Bel Fdhila and Duineveld, 1996). All simulations have been performed with a standard PC (AMD Athlon XP3000 processor, 2.17 GHz with 1 GB RAM).
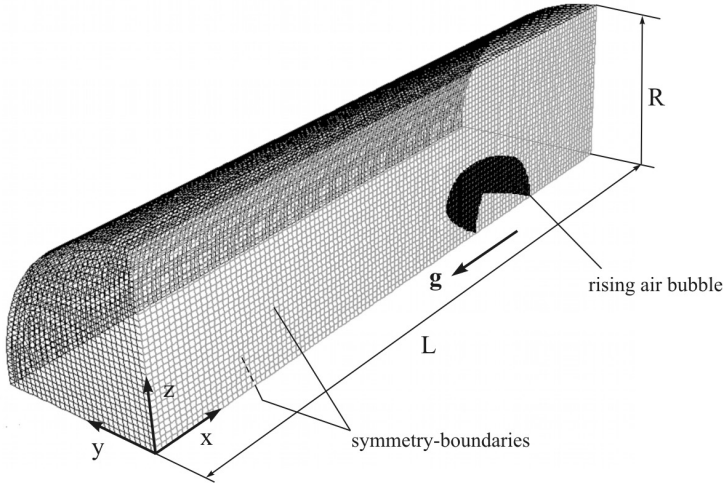
Figure 6: Computational domain with hybrid grid (85080 computational cells)

Table 1: Parameter of used surfactant

initial volume concentration	$c_0 = 4,443 \cdot 10^{-4} mol\ m^{-3}$
bulk diffusion coefficient	$D = 2,7 \cdot 10^{-10} m^2 s^{-1}$
surface diffusion coefficient	$D^\Sigma = 10^{-9} m^2 s^{-1}$,
maximum surface excess concentration	$\Gamma_\infty = 2,91 \cdot 10^{-6} mol^2 m^{-2}$
Langmuir coefficient	$b = 6,63 \cdot 10^{-4} mol\ m^{-3}$

4.2 Simulation results

With the numerical method introduced above, the surfactant distribution in the bulk phase and on the interface and the induced Marangoni stresses have been simulated. Figure 8 shows the surfactant distribution on the bubble surface. The equilibrium value corresponding to the initial bulk concentration c_0 is $\Gamma_{eq}(c_0) = 1.17 \cdot 10^{-6} mol/m^2$. In accordance with the literature, the surfactant accumulates at the rear pole where the maximum surface excess concentration Γ_∞ is reached. Inside a large region at the front side of the bubble the surface excess concentration is much less than $\Gamma_{eq}(c_0)$. Between these two regions, a small transition zone is formed. Figure 9a shows the distribution of the bulk concentration of the dissolved surfactant; here the bubble moves from the left to the right. During its rise, the bulk concentration becomes significantly higher (with $1.79 \cdot 10^{-1} mol/m^3$ about 400 times of the initial concentration) behind the rear pole of the bubble due to desorption of surfactant. In Figure 9b, the region with a surfactant concentration
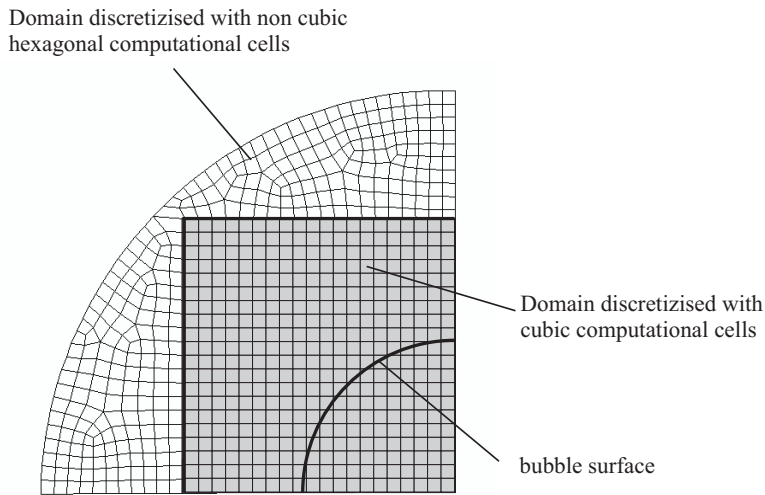
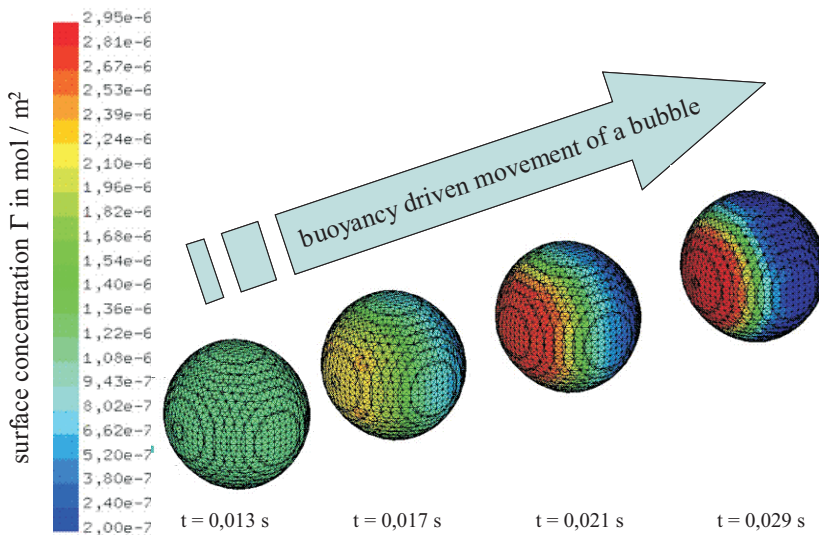Figure 7: Discretization of the pipe cross section

Figure 8: Distribution of the adsorbed surfactant on a bubble surface

below the initial concentration c_0 is depicted. In front of the bubble, the bulk concentration of the surfactant is nearly zero. With larger distance from the bubble surface, the concentration increases. Due to this concentration gradient normal to

the bubble surface, the dissolved surfactant is transported to the interface via molecular diffusion. Due to the surface gradient of the surface excess concentration and
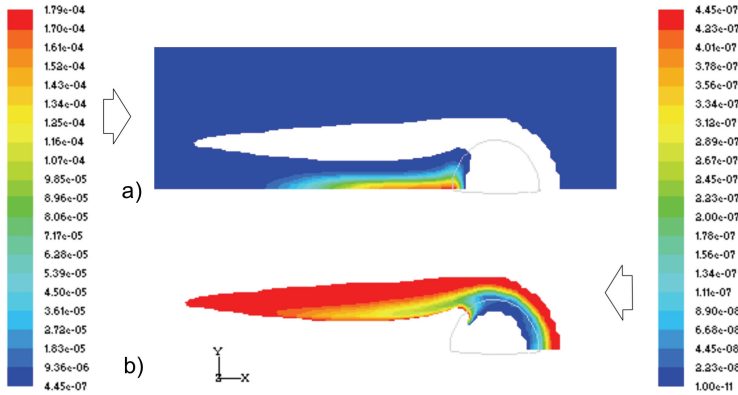

Figure 9: Concentration of dissolved surfactant

the surface equation of state, a surface tension gradient is formed according to (12). This Marangoni stress affects the mobility of the interface and, thereby, the velocity field inside and outside the particle. This is shown in Figure 10, where the relative velocity fields (with respect to the bubble's barycenter) are presented for a bubble rising in a pure liquid (left) and in a surfactant solution (right), respectively. In both cases the terminal velocity has already been reached. In the pure system only one toroidal vortex is formed inside the bubble whereas two vortices are formed if surfactant is present. In the latter case the interfacial velocity at the rear pole is oriented against the direction of the bubble's movement. Tasoglu, Demirci, and Muradoglu (2008) also obtained two vortices inside the bubble in the simulations using a nonlinear surface equation of state derived from the Langmuir adsorption isotherm if the surface elasticity number and the Peclet number based on the bulk surfactant diffusivity are sufficient high. The conditions under which a secondary vortex is formed inside the fluid particle will be examined in further studies. Furthermore, the bubble is more flattened than in the surfactant solution because of the different rise velocities. Due to the "reverse flow" at the rear pole, the velocity gradient and therewith the viscous friction force is increased in the surfactant solution. Figure 11 shows a plot of the rise velocities versus time, calculated without and with the Marangoni stress term, respectively. The simulation results reflect the known retardation induced by surfactants. Without any hydromechanical back-coupling, i.e. for constant surface tension $\sigma \equiv \sigma_0 = 30\ mN/m$, a terminal velocity
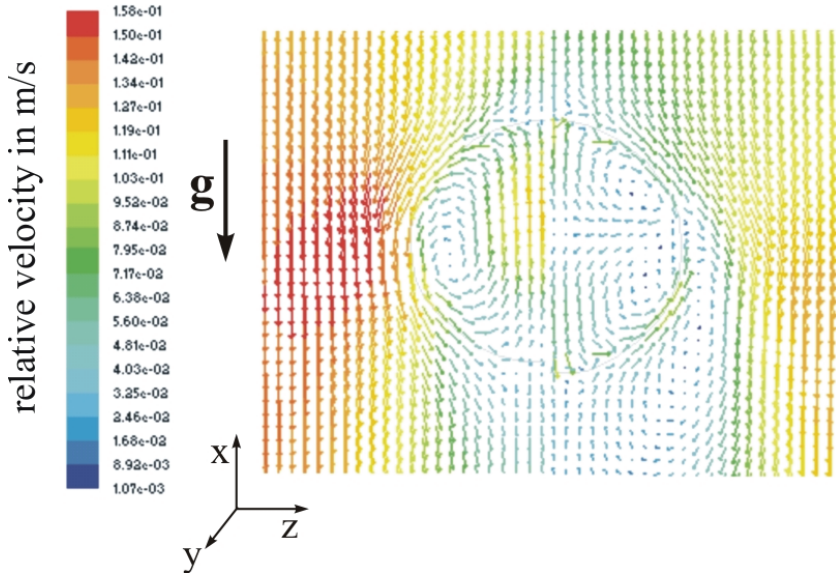
Figure 10: Velocity field inside and outside the bubble rising a pure system (left) and in a diluted surfactant solution (right)

of about 12 cm/s is reached (upper curve in Figure 11). The Marangoni stress term $\nabla_\Sigma \sigma$, obtained with a linear surface equation of state according to

$$\sigma(\Gamma) = \sigma_0 - a\frac{\Gamma}{\Gamma_\infty} \quad \text{for} \quad \Gamma \le \Gamma_\infty \quad \text{with} \quad a = 0.01 N/m \tag{38}$$

alone, reduces already the terminal velocity to 8,5 cm/s. Here, in the curvature term, the surface tension is kept constant to $\sigma \equiv \sigma_0$. Note that the back-coupling is switched on only after a rise velocity of 10 cm/s is reached. This is necessary with the used solver because so-called parasitic currents prevent the correct simulation of the interfacial surfactant transport at the beginning of the simulation. The lower curve in Figure 11 is obtained using (38) both in the capillary and the Marangoni stress term. In this case the retardation is even more pronounced because the lower surface tension leads to a stronger deformation of the bubble. To reduce computational time, each simulation was stopped when the rise velocity became stable.
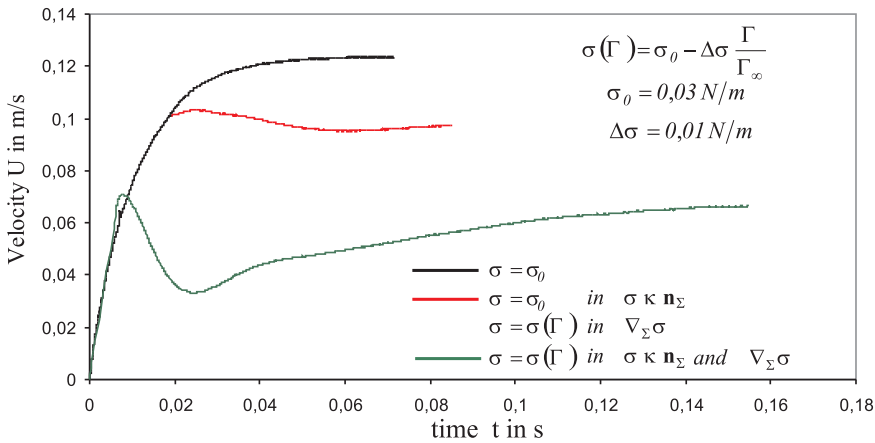
Figure 11: Effect of hydrodynamical back-coupling on the rising velocity of the bubble

5 Conclusion

A new VOF-based approach for simulating the influence of a soluble surfactant on the dynamical behavior of a fluid particle in 3D is introduced. The numerical method yields both the surfactant distribution in the bulk phase and on the interface and accounts for the induced Marangoni stress acting on the interface. It applies to systems with fast sorption where the interfacial surfactant concentration is related to the adjacent bulk concentration via an adsorption isotherm. In this case only bulk values for the surfactant concentrations are required, provided that the discretized interfacial transport terms are appropriately corrected to compensate induced artificial fluxes. First numerical results concerning an air bubble rising in a quiescent surfactant solution reflect the known retardation of the bubble. Since the approach is based on the Volume of Fluid method, the simulation of two-phase flows with changes in phase topology like disintegration processes or bubble and droplet formation at nozzles is possible.

References

Alke, A. (2008): *Numerische Modellierung des Einflusses löslicher Tenside auf fluide Zweiphasensysteme*. PhD thesis, University of Paderborn, Germany, 2008.

Alke, A.; Bothe, D. (2007):   A VOF-simulation of fluid particles influenced by soluble surfactants. In *6th International Conference on Multiphase Flow, ICMF2007, paper S1ThuC57*.

Bazhlekov, I.; Anderson, P. D.; Meijer, H. E. E. (2004):   Boundary integral method for deformable interfaces in the presence of insoluble surfactants.   *Lect. Notes Comput. Sci.*, vol. 2907, pp. 355 – 362.

Bazhlekov, I.; Anderson, P. D.; Meijer, H. E. E. (2006):   Numerical investigation of the effect of insoluble surfactants on drop deformation and breakup in simple shear flow.   *J. Colloid Interface Sci.*, vol. 298, pp. 369 – 394.

Bel Fdhila, R.; Duineveld, P. (1996):   The effect of surfactant on the rise of a spherical bubble at high Reynolds and Peclet numbers.   *Phys. Fluids*, vol. 8, no. 2, pp. 310 – 321.

Bothe, D.; Prüss, J.; Simonett, G. (2005):   Well-posedness of a two-phase flow with soluble surfactant. In Chipot, M.; Escher, J.(Eds):   *Nonlinear elliptic and parabolic problems*, no. 64 in Progress in nonlinear differential equations and their applications, pp. 37 – 61, Basel. Birkhäuser.

Brackbill, J.; Kothe, D.; Zemach, C. (1992):   A continuum method for modeling surface tension.   *J. Comp. Phys.*, vol. 100, pp. 335 – 354.

Cermelli, R.; Fried, E.; Gurtin, M. (2005):   Transport relations for surface integrals arising in the formulation of balance laws for evolving fluid interfaces.   *J. of Fluid Mech.*, vol. 544, pp. 339 – 351.

Davidson, M.; Harvie, D. (2007):   Predicting the effect of interfacial flow of insoluble surfactant on the deformation of drops rising in a liquid.   *ANZIAM J.*, vol. 48, pp. C661 – C676.

Davis, R.; Acrivos, A. (1966):   The influence of surfactants on the creeping motion of bubbles.   *Chem. Eng. Sci.*, vol. 21, pp. 681 – 685.

Drumright-Clarke, M.; Renardy, Y. (2004):   The effect of insoluble surfactant at dilute concentration on drop breakup under shear with inertia.   *Phys. Fluids*, vol. 16, pp. 14 – 21.

Edwards, D. A.; Brenner, H.; Wasan, D. (1991):   *Interfacial transport processes and rheology*. Butterworth-Heinemann.

Feigl, K.; Megias-Alguacil, D.; Fischer, P.; Windhab, E. (2007):   Simulation and experiments of droplet deformation and orientation in simple shear flow with surfactants.   *Chem. Eng. Sci.*, vol. 62, pp. 3242 – 3258.

Gurtin, M.; Struthers, A.; Williams, W. (1989): A transport theorem for moving interfaces. *Quart. of Appl. Math.*, vol. 47, no. 4, pp. 773 – 777.

Harper, J. (1973): On bubbles with small immobile adsorbed films rising in liquids at low Reynolds numbers. *J. Fluid Mech.*, vol. 58, pp. 539 – 545.

Harper, J. (1982): Surface activity and bubble motion. *Appl. Sci. Res.*, vol. 38, pp. 343 – 352.

He, Z.; Malsrelli, C.; Dagan, Z. (1990): The size of stagnant caps of soluble surfactant on the interfaces of translating fluid droplets. *J. Colloid Interface Sci.*, vol. 146, no. 2, pp. 442 – 451.

James, A.; Lowengrub, J. (2004): A surfactant-conserving volume-of-fluid method for interfacial flows with insoluble surfactant. *J. Comp. Phys.*, vol. 201, pp. 685 – 722.

Johnson, R.; Borhan, A. (1996): Stability of the shape of a surfactant-laden drop translating at low Reynolds number. *Phys. Fluids*, vol. 12, pp. 773 – 784.

Khattari, Z.; Steffen, P.; Fischer, T. M. (2002): Migration of a droplet in a liquid: effect of insoluble surfactants and thermal gradient. *J. Phys.: Condens. Matter*, vol. 214, pp. 4823 – 4828.

Kruijt-Stegeman, Y.; van de Vosse, F.; Meijer, H. (2004): Droplet behavior in the presence of insoluble surfactant. *Phys. Fluids*, vol. 16, pp. 2785 – 2796.

Levan, M. D.; Newman, J. (1976): The effect of surfactant on the terminal and interfacial velocities of a bubble or drop. *AIChE J.*, vol. 22, no. 4, pp. 695 – 701.

Li, X.; Pozrikidis, C. (1997): The effect of surfactants on drop deformation and on the rheology of dilute emulsions in Stokes flow. *J. Fluid Mech.*, vol. 341, no. 4, pp. 1365 – 194.

Li, X.-J.; Mao, Z. (2001): The effect of surfactant on the motion of a buoyancy-driven drop at intermediate Reynolds numbers: a numerical approach. *J. Colloid Interface Sci.*, vol. 240, pp. 307 – 322.

Liao, Y.-C.; Franses, E.; Barasan, O. (2003): Computation of dynamic adsorption with adaptive integral, finite difference, and finite element methods. *J. Colloid Interface Sci.*, vol. 258, pp. 310 – 321.

Milliken, W. J.; Stone, H. A.; Leal, L. G. (1993): The effects of surfactants on transient motion of Newtonian drops. *Phys. Fluids A*, vol. 5, pp. 69 – 79.

Muradoglu, M.; Tryggvason, G. (2008): A front-tracking method for computation of interfacial flows with soluble surfactants. *J. Comp. Phys.*, vol. 227, pp. 2238 – 2262.

Pozrikidis, C. (2001): Interfacial dynamics for Stokes flow. *J. Comp. Phys.*, vol. 169, pp. 250 – 301.

Ravera, F.; Ferrari, M.; Liggieri, L. (2000): Adsorption and partitioning of surfactants in liquid-liquid systems. *Adv. Colloid Interface Sci.*, vol. 88, pp. 129 – 177.

Renardy, Y.; Renardy, M.; Cristini, V. (2002): A new volume-of-fluid formulation for surfactants and simulations of drop deformation under shear at low viscosity ratio. *Eur. J. Mech.- B Fluids*, vol. 21, pp. 49 – 59.

Rudman, M. (1998): A volume tracking method for interfacial flows with large density variations. *Int. J. Numer. Meth. Fluids*, vol. 28, pp. 357 – 378.

Savic, P. (1953): Circulation and distortion of liquid drops falling through a viscous medium. Technical Report MT-22, Nat. Res. Coun. Canada, Div. Mech. Eng., 1953.

Schlüter, M. (2002): *Blasenbewegung in praxisrelevanten Zweiphasenströmungen, VDI Fortschritt-Bericht Nr. 432*. VDI-Verlag, Düsseldorf.

Severino, M.; Campana, D.; Giavedoni, M. (2005): Effects of surfactant on the motion of a confined gas-liquid interface. The influence of the Peclet number. *Lat. Am. Appl. Res.*, vol. 35, pp. 225 – 232.

Slattery, J.; Sagis, J. L.; Oh, E.-S. (2007): *Interfacial Transport Phenomena*. Springer, Berlin.

Tasoglu, S.; Demirci, U.; Muradoglu, M. (2008): The effect of soluble surfactant on the transient motion of a buayancy-driven bubble. *Phys. Fluids*, vol. 20.

Wasserman, M. L.; Slattery, J. C. (1969): Creeping flow past a fluid globule when a trace of surfactant is present. *AIChE J.*, vol. 15, no. 4, pp. 533 – 547.

Xu, J.-J.; Li, Z.; Lowengrub, J.; Zhao, H. (2006): A level-set method for interfacial flows with surfactant. *J. Comp. Phys.*, vol. 212, pp. 590 – 616.

Yamamoto, Y.; Yamauchi, M.; Uemura, T. (2006): Numerical simulation of a contaminated droplet by front-tracking method taking the effect of surfactant on the interface. In *Proceeding of FEDSM2006, 2006 ASME Joint U.S.-European Fluids Eng. Conf.*, Miami, USA.

Yang, X.; James, A. (2007): An arbitrary lagrangian-eulerian (ale) method for interfacial flows with insoluble surfactants. *FDMP: Fluid Dynamics & Materials Processing*, vol. 3, no. 1, pp. 65–96.

Youngs, D. (1982): Time-dependent multi-material flow with large fluid distortion. In Morton, K.; Bains, M. G.(Eds): *Numerical Methods for Fluid dynamics*, pp. 273 – 285. Academic Press.

Zhang, J.; Eckmann, D.; Ayyaswamy, P. (2006): A front tracking method for a deformable intravascular bubble in a tube with soluble surfactant transport. *J. Comp. Phys.*, vol. 214, pp. 366 – 396.

Appendix A: Transport theorem for a moving surface cut by a fixed volume

The transport theorem for the rate of change of an extensive surface quantity Φ^Σ on a material surface $\Sigma_m(t)$ states that

$$\frac{d\Phi^\Sigma}{dt} = \frac{d}{dt}\int_{\Sigma_m(t)} \phi^\Sigma \, dA = \int_{\Sigma_m(t)} \left(\frac{D\phi^\Sigma}{Dt} + \phi^\Sigma \, \nabla_\Sigma \cdot \mathbf{u} \right) dA, \tag{39}$$

where $\frac{D}{Dt}$ is the Lagrangian derivative and ϕ^Σ the area density of Φ^Σ. For the rate of change of a surface quantity on the part of a moving surface lying inside a fixed volume V the change due to the surface movement has to be taken into account. During a time interval of length dt, the moving surface - and with it the surface quantity - partly enters and partly leaves the cell. Therefore, the ingoing amount of Φ^Σ has to be added to and the outgoing part has to be subtracted from the right-hand side of (39). This additional kinematic term can be derived from simple geometric considerations illustrated by Figure 12 where the bold part of the surface with length

$$\frac{\mathbf{u} \cdot \mathbf{n}}{sin\alpha} \Delta t = \frac{\mathbf{u} \cdot \mathbf{n}}{\sqrt{1 - cos^2\alpha}} \Delta t = \frac{\mathbf{u} \cdot \mathbf{n}}{\sqrt{1 - (\mathbf{n} \cdot \mathbf{n}_\Sigma)^2}} \Delta t \tag{40}$$

leaves the cell across the right cell boundary during the time interval Δt. The resulting rate at which surface leaves the volume V is obtained by integration of the above rate $\mathbf{u} \cdot \mathbf{n}/\sqrt{1 - (\mathbf{n} \cdot \mathbf{n}_\Sigma)^2}$ along the curve of intersection between the surface and the boundary of V. This leads to an extended version of the transport theorem, given as

$$\frac{d}{dt}\int_{\Sigma(t) \cap V} \phi^\Sigma \, dA = \int_{\Sigma(t) \cap V} \left(\frac{D\phi^\Sigma}{Dt} + \phi^\Sigma \, \nabla_\Sigma \cdot \mathbf{u} \right) dA$$

$$- \int_{\partial(\Sigma(t) \cap V)} \phi^\Sigma \frac{\mathbf{u} \cdot \mathbf{n}}{\sqrt{1 - (\mathbf{n} \cdot \mathbf{n}_\Sigma)^2}} \, ds. \tag{41}$$
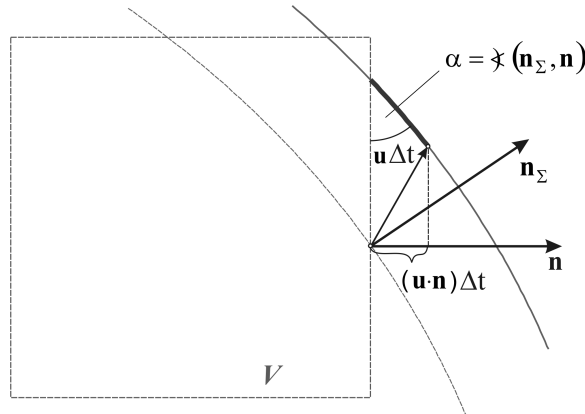
Figure 12: Illustration of the extended surface transport theorem

Equation (41) is very close to the formula given in Remark 3 in (Gurtin, Struthers, and Williams, 1989) but the latter is flawed by a misprint. Note that (41) is consistent with the recent general form of surface transport relations given in (Cermelli, Fried, and Gurtin, 2005).

Appendix B: Total surfactant mass balance for a fixed control volume cut by a moving interface

The total (molar) mass balance for a soluble surfactant within a material volume $V(t)$ is given by

$$\frac{d}{dt}\left[\int_{V(t)} c\, dV + \int_{\Sigma(t)\cap V(t)} \Gamma\, dA\right] = -\int_{\partial V(t)} \mathbf{j}\cdot\mathbf{n}\, dA - \int_{\partial(\Sigma(t)\cap V(t))} \mathbf{j}^{\Sigma}\cdot\mathbf{N}\, ds. \qquad (42)$$

For a fixed control volume V, as used for the Finite Volume discretization, the convective fluxes have to be accounted for. In the following, surfactant is assumed to be soluble only inside phase Ω^{+}. Application of the Reynolds transport theorem to the concentration c and use of the local surfactant balance (1) yields the rate of change of dissolved surfactant inside a fixed volume V, containing a part of the interface, as

$$\frac{d}{dt}\int_{V\cap\Omega^{+}(t)} c\, dV = -\int_{\partial V\cap\Omega^{+}(t)} (c\,\mathbf{u}+\mathbf{j})\cdot\mathbf{n}\, dA + \int_{\Sigma(t)\cap V} \mathbf{j}\cdot\mathbf{n}_{\Sigma}\, dA. \qquad (43)$$

According to the extended version of the surface transport theorem (41), the rate of change of the adsorbed surfactant inside V is

$$\frac{d}{dt} \int_{\Sigma(t) \cap V} \Gamma \, dA = \int_{\Sigma(t) \cap V} \left(\frac{D\Gamma}{Dt} + \Gamma \nabla_\Sigma \cdot \mathbf{u} \right) dA$$

$$- \int_{\partial(\Sigma(t) \cap V)} \Gamma \frac{\mathbf{u} \cdot \mathbf{n}}{\sqrt{1 - (\mathbf{n} \cdot \mathbf{n}_\Sigma)^2}} \, ds. \tag{44}$$

The integrand of the first term on the right-hand side of (44) can be expressed by the local balance of adsorbed surfactant (2). Application of the surface divergence theorem to the molecular interfacial flux $\mathbf{j}^\Sigma$ and use of the interfacial sorption condition (5) gives

$$\frac{d}{dt} \int_{\Sigma(t) \cap V} \Gamma \, dA = - \int_{\Sigma(t) \cap V} \mathbf{j} \cdot \mathbf{n}_\Sigma \, dA - \int_{\partial(\Sigma(t) \cap V)} \mathbf{j}^\Sigma \cdot \mathbf{N} \, ds$$

$$- \int_{\partial(\Sigma(t) \cap V)} \Gamma \frac{\mathbf{u} \cdot \mathbf{n}}{\sqrt{1 - (\mathbf{n}_\Sigma \cdot \mathbf{n})^2}} \, ds. \tag{45}$$

Addition of (43) and (45) finally yields

$$\frac{d}{dt} \left[\int_{V \cap \Omega^+(t)} c \, dV + \int_{\Sigma(t) \cap V} \Gamma \, dA \right] = - \int_{\partial V \cap \Omega^+(t)} (c \, \mathbf{u} + \mathbf{j}) \cdot \mathbf{n} \, dA$$

$$- \int_{\partial(\Sigma(t) \cap V)} \mathbf{j}^\Sigma \cdot \mathbf{N} \, ds - \int_{\partial(\Sigma(t) \cap V)} \Gamma \frac{\mathbf{u} \cdot \mathbf{n}}{\sqrt{1 - (\mathbf{n}_\Sigma \cdot \mathbf{n})^2}} \, ds. \tag{46}$$

Appendix C: Derivation of the source term $\dot{S}$

According to the Reynolds transport theorem, the rate of change of the amount of surfactant, dissolved in Ω^+, in a fixed control volume V is

$$\frac{d}{dt} \int_{V \cap \Omega^+(t)} \tilde{c} \, dV = \int_{V \cap \Omega^+(t)} \frac{\partial \tilde{c}}{\partial t} \, dV - \int_{V \cap \Sigma(t)} \tilde{c} \mathbf{u} \cdot \mathbf{n}_\Sigma \, dA. \tag{47}$$

Use of the local balance equation (1) and the divergence theorem yields

$$\frac{d}{dt} \int_{V \cap \Omega^+(t)} \tilde{c} \, dV = - \int_{\partial V \cap \Omega^+(t)} \left(\tilde{c} \mathbf{u} + \tilde{\mathbf{j}} \right) \cdot \mathbf{n} \, dA + \int_{\Sigma(t) \cap V} \left(\tilde{c} \mathbf{u} + \tilde{\mathbf{j}} \right) \cdot \mathbf{n}_\Sigma \, dA$$

$$- \int_{\Sigma(t) \cap V} \tilde{c} \mathbf{u} \cdot \mathbf{n}_\Sigma \, dA, \tag{48}$$

hence, with the homogeneous Neumann condition $\widetilde{\mathbf{j}} \cdot \mathbf{n}_\Sigma = 0$ on $\Sigma(t)$,

$$
\frac{d}{dt} \int_{V \cap \Omega^+(t)} \widetilde{c} \, dV = - \int_{\partial V \cap \Omega^+(t)} \left(\widetilde{c} \mathbf{u} + \widetilde{\mathbf{j}} \right) \cdot \mathbf{n} \, dA. \tag{49}
$$

Further, the extended surface transport theorem (41) applied to $g(\widetilde{c})$ yields

$$
\frac{d}{dt} \int_{\Sigma(t) \cap V} g(\widetilde{c}) \, dA = \int_{\Sigma(t) \cap V} \left(\frac{D}{Dt} g(\widetilde{c}) + g(\widetilde{c}) \, \nabla_\Sigma \cdot \mathbf{u} \right) dA
$$
$$
- \int_{\partial(\Sigma(t) \cap V)} g(\widetilde{c}) \, \frac{\mathbf{u} \cdot \mathbf{n}}{\sqrt{1 - (\mathbf{n}_\Sigma \cdot \mathbf{n})^2}} \, ds. \tag{50}
$$

Addition of (49) and (50) gives

$$
\frac{d}{dt} \left[\int_{V \cap \Omega^+(t)} \widetilde{c} \, dV + \int_{\Sigma(t) \cap V} g(\widetilde{c}) \, dA \right]_{\mathbf{j} \cdot \mathbf{n}_\Sigma = 0} = - \int_{\partial V \cap \Omega^+(t)} \left(\widetilde{c} \mathbf{u} + \widetilde{\mathbf{j}} \right) \cdot \mathbf{n} \, dA
$$
$$
+ \int_{\Sigma(t) \cap V} \left(\frac{D}{Dt} g(\widetilde{c}) + g(\widetilde{c}) \nabla_\Sigma \cdot \mathbf{u} \right) dA - \int_{\partial(\Sigma(t) \cap V)} g(\widetilde{c}) \, \frac{\mathbf{u} \cdot \mathbf{n}}{\sqrt{1 - (\mathbf{n}_\Sigma \cdot \mathbf{n})^2}} \, ds. \tag{51}
$$

The first and the third term on the right-hand side of (51) also appear in the balance equation (15). Therefore, the rate of change of the total amount of surfactant in a computational cell can be calculated as

$$
\frac{d}{dt} \left[\int_{V \cap \Omega^+(t)} c \, dV + \int_{\Sigma(t) \cap V} \Gamma \, dA \right] =
$$
$$
\frac{d}{dt} \left[\int_{V \cap \Omega^+(t)} \widetilde{c} \, dV + \int_{\Sigma(t) \cap V} g(\widetilde{c}) \, dA \right]_{\mathbf{j} \cdot \mathbf{n}_\Sigma = 0} + \dot{S}, \tag{52}
$$

where

$$
\dot{S} = - \int_{\partial(\Sigma(t) \cap V)} \mathbf{j}^\Sigma \cdot \mathbf{N} \, ds - \int_{\Sigma(t) \cap V} \left(\frac{D}{Dt} g(\widetilde{c}) + g(\widetilde{c}) \nabla_\Sigma \cdot \mathbf{u} \right) dA. \tag{53}
$$

This source term corrects the "ghost flux" along the interface induced by the bulk transport of dissolved surfactant via the local equilibrium relation $\Gamma = g(\widetilde{c})$.